THE JOURNAL OF PHYSICAL CHEMISTRY Letters

Letter

pubs.acs.org/JPCL

How Important Is the Organic Part of Lead Halide Perovskite Photovoltaic Cells? Efficient $CsPbBr_3$ Cells

Michael Kulbak, David Cahen,* and Gary Hodes*

Department of Materials and Interfaces, Weizmann Institute of Science, Rehovot 76100, Israel

Supporting Information

ABSTRACT: Hybrid organic–inorganic lead halide perovskite photovoltaic cells have already surpassed 20% conversion efficiency in the few years that they have been seriously studied. However, many fundamental questions still remain unanswered as to why they are so good. One of these is "Is the organic cation really necessary to obtain high quality cells?" In this study, we show that an all-inorganic version of the lead bromide perovskite material works equally well as the organic one, in particular generating the high open circuit voltages that are an important feature of these cells.

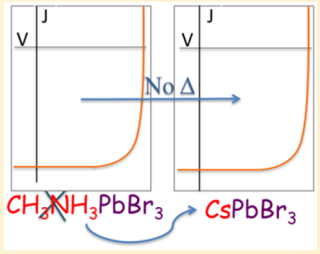

Organic amine-lead-halide perovskite-based photovoltaic cells have become one of the most studied cells, if not *the* most studied, as well as being highly promising for practical applications, all in the past several years. These cells are commonly called "hybrid organic–inorganic perovskite cells". However, much early work on these or related materials (not related to photovoltaic cells) involved totally inorganic lead halide compounds with alkali metal ions as the 'A' cation in the generalized $APbX_3$ (X = halide) compound. Although all top-performing photovoltaic cells used alkyl ammonium or formamidinium as the A cation, we query as to whether an inorganic A cation would also form light absorbers with comparable properties to the alkyl ammonium ones. Some indirect evidence already provides strong support that this may be the case. For charge transport, the two most relevant parameters are charge mobility (directly related to diffusion coefficient) and lifetime, which, taken together, define the carrier diffusion/drift length. $CsSnI_3$ has been reported with high mobilities of electrons (up to ~2300 $cm^2/V{\cdot}s$) and holes (~320 $cm^2/V{\cdot}s$).[1] We are aware of two studies of photovoltaic cells using $CsSnI_3$ as an absorber: an early report (2012) used in a planar Schottky cell configuration[2] with a modest performance (0.9% efficiency) and a more recent one with an improved, but still low (compared to Pb perovskites) performance of 2% efficiency.[3] More specifically, in a study of $CsPbBr_3$ single crystals for use as photoconductive X- and γ-ray detectors, Stoumpos et al. estimated an electron mobility of ~1000 $cm^2/V{\cdot}s$ and an electron lifetime of 2.5 μs (and comparable $\mu\tau$ values for electrons and holes).[4] From these parameters, it is clear that the organic cation is not necessarily essential to obtain long diffusion/drift lengths. However, one of the outstanding properties of the hybrid perovskites is the very high value of open circuit voltage (V_{OC}) that can be obtained relative to the semiconductor bandgap. In addition to mobility and lifetimes, other factors are important to obtain high V_{OC}, e.g., minimal tail absorption as broad tail absorption will reduce the available V_{OC}.

To find out whether the organic nature or anisotropic geometry of the A cation is essential for the high performance of the hybrid cells, we chose $CsPbBr_3$ because, unlike the iodide compound, this material occurs at standard temperature and pressure in the perovskite structure and was shown to have very good charge transport properties.[4] In this Letter, we show that $CsPbBr_3$ exhibits a photovoltaic performance comparable to that obtained by $CH_3NH_3PbBr_3$ (abbreviated here to $MAPbBr_3$), including relatively high values of V_{OC} typical of the hybrid perovskites.

To prepare the $CsPbBr_3$ layers, we used the two-step method, since (based on attempts with a few different solvents and excluding concentrated aqueous HBr as used in ref 4 to prepare starting material as being inconvenient for spin-coating) we were unable to find a solvent that dissolved both the CsBr and the $PbBr_2$; also the morphology obtained with the two-step method for $MAPbBr_3$ is more homogeneous and continuous than that from the one-step method.[5] The $CsPbBr_3$ layers were annealed at 250 °C and the cells fabricated in ambient atmosphere. The relatively high annealing temperature and the fact that all processing was carried out in ambient atmosphere implies a fairly good stability, although, like the hybrid perovskites, liquid water will cause rapid degradation.

We studied various cell architectures, i.e., with mesoporous (mp)-TiO_2, with mp-Al_2O_3 and without mp layer (planar). Since cells with mp-TiO_2 gave by far the best overall results, we concentrated on the architecture F-doped tin oxide (FTO)/TiO_2(dense)/mp-TiO_2/$CsPbBr_3$/HTM/Au (where HTM represents hole transport medium), and all cells below are of this configuration unless stated otherwise. To maximize V_{OC}, we used several different HTMs, i.e., spiro-OMeTAD, poly[bis(4-phenyl)(2,4,6-trimethylphenyl)amine], and 4,4′-bis(N-carbazolyl)-1,1′-biphenyl; abbreviated as spiro, PTAA and CBP,

Received: May 10, 2015
Accepted: June 10, 2015
Published: June 10, 2015

DOI: 10.1021/acs.jpclett.5b00968
J. Phys. Chem. Lett. 2015, 6, 2452–2456

respectively. The highest occupied molecular orbital (HOMO) level of the HTM is an important factor in maximizing V_{OC}—ideally it should be slightly closer to the vacuum level, E_{vac} (i.e., slightly lower ionization energy, IE) than the top of the valence band (E_V) of the perovskite. We measured by ultraviolet photoelectron spectroscopy (UPS) E_V of our $CsPbBr_3$ on mp TiO_2 to be at 5.97 eV (vs the E_{vac}) which is very similar to the 5.9 eV we previously measured for $MAPbBr_3$.[6] Most common HTMs have E_V/IE values considerably closer to E_{vac} than this. For spiro, PTAA, and CBP, the values are ~5.0 eV,[6] ~ 5.2 eV,[7,8] and ~5.7 eV,[9] respectively. As always, these values may change, dependent on processing, ambient conditions, and when contacted with another material, and should be taken as a guide rather than as exact numbers.

Figure 1 shows a transmission spectrum (corrected for reflection) of $CsPbBr_3$ on mp-TiO_2/FTO glass. Attempts to

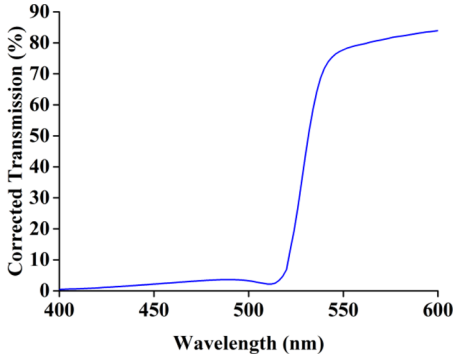

Figure 1. Reflection-corrected transmission of $CsPbBr_3$ on mp-TiO_2 (effective $CsPbBr_3$ thickness ca. 400−500 nm; see SEM image in Figure 2).

calculate a bandgap from Tauc plots (Figures S1a and S1b in the Supporting Information (SI)) gave a direct gap of 2.36 eV (compared to 2.32 for the $MAPbBr_3$[10]). However, at this energy, there is already a 2/3 drop in transmission, implying a different absorption process at energies lower than 2.36 eV. Fitting the Tauc plot to an indirect gap gave a linear range from ~2.35−2.40 eV with an extrapolated indirect gap of ~2.29 eV. Based on a visual inspection of the transmission spectrum and assuming a direct gap, an estimated gap of 2.32 ± 0.02 is estimated. It may be that there is an indirect gap followed closely by a direct gap. While an indirect gap is not usually sharp, this need not necessarily always be the case. There also may be an excitonic contribution. A study of the absorption of this material will be the subject of future work and the bandgaps given here should be considered an estimation. It should be noted that Stoumpos et al. measured a direct gap of 2.25 eV[4] for their single crystal $CsPbBr_3$. Recently, several independent measurements of single crystal hybrid perovskites yielded bandgap values about 0.1 eV lower than those widely accepted for films of the same compounds.[11,12]

The X-ray diffraction (XRD, Figure S2 in the SI) pattern matches exactly that given in the literature for this compound.[4] Figure 2 shows a scanning electron microscopy (SEM) image of a cross-section of a cell with spiro as the HTM. The mp-TiO_2/$CsPbBr_3$ and spiro layers are each ~450 nm thick, while the $CsPbBr_3$ overlayer averages ~270 nm thick.

Spiro was first used, as it is expected to give good cells with bromide perovskites relative to many other HTMs, although with a lower V_{OC} than can be achieved with optimal interfacial

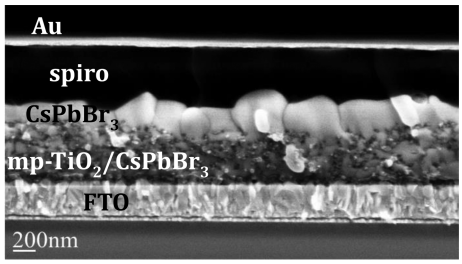

Figure 2. SEM cross-section of a mp-TiO_2/$CsPbBr_3$/spiro/Au cell. The dense TiO_2 on the FTO is not clearly visible in this image.

energy level alignment. This follows from the lower IE of spiro compared to the other HTMs used here (as also pointed out in ref 6) although there are some recent results showing high V_{OC} with spiro (see Table S1 in the SI). Figure 3 shows the I−V characteristics of cells with different HTMs as well as without a HTM.

Considering first the spiro cell (Figure 3A), high currents and fill factors (FF) with moderate voltages were obtained. The lower values of V_{OC} than obtained in high voltage $MAPbBr_3$ cells using larger IE HTMs (which can give up to 1.5 V) are reasonable considering that spiro is known to be suboptimal for this parameter. Additionally there is a small hysteresis and only between the maximum power range and open-circuit. This is not a temperature effect (as a rule of thumb, photovoltaic cells lose ~2 mV in V_{OC} for every °C rise in temperature[13] since (a) the cells were allowed to equilibrate before measuring and (b) the forward scan was run first followed by the reverse scan, which would imply a higher V_{OC} for forward scan in the case where temperature equilibrium was not reached.

Based solely on its HOMO level, PTAA should give somewhat higher values of V_{OC} than spiro. Indeed >25% higher V_{OC} values were obtained in first experiments, as can be seen from Figure 3B. The nearly 1.3 V V_{OC} did not change the FF, although there was a ~ 8% drop in current, likely due to suboptimal doping of the HTM. The hysteresis was slightly smaller, relative to that of the cells with spiro, and in this case was manifested mainly by a small change in the cell resistance. We note that some of these cells show virtually no hysteresis at all.

The maximum current that can be obtained for 100% EQE for a bandgap of 2.36 eV is ~9 mA/cm^2. The EQE values (without light bias) shown in Figure 4 translate to a current density of ~5.5 mA/cm^2, which is slightly more than 10% lower than the directly measured J_{SC} with PTAA as the hole conductor (Figure 3B).

Cells were also measured in natural sunlight (900 W/m^2). Correcting for the difference between 900 W/m^2 and the 1000 W/m^2 of the simulator, the J_{SC} values were very similar. Measurements of EQE with white light bias, which often influences the values of EQE, increases the EQE to close to 70%. Such an EQE value yields an equivalent J_{SC} that agrees with the directly measured result (Figure 3B), even though the white light source used for this purpose was much weaker than the natural sunlight. In this respect, it is worth noting that we recently showed that weak white light illumination increases the effective diffusion length of charge carriers in $MAPbBr_3$ by up to a factor of 3 when measured by electron beam-induced current (EBIC)[14] and there may well be a connection between these two different results.

DOI: 10.1021/acs.jpclett.5b00968
J. Phys. Chem. Lett. 2015, 6, 2452−2456

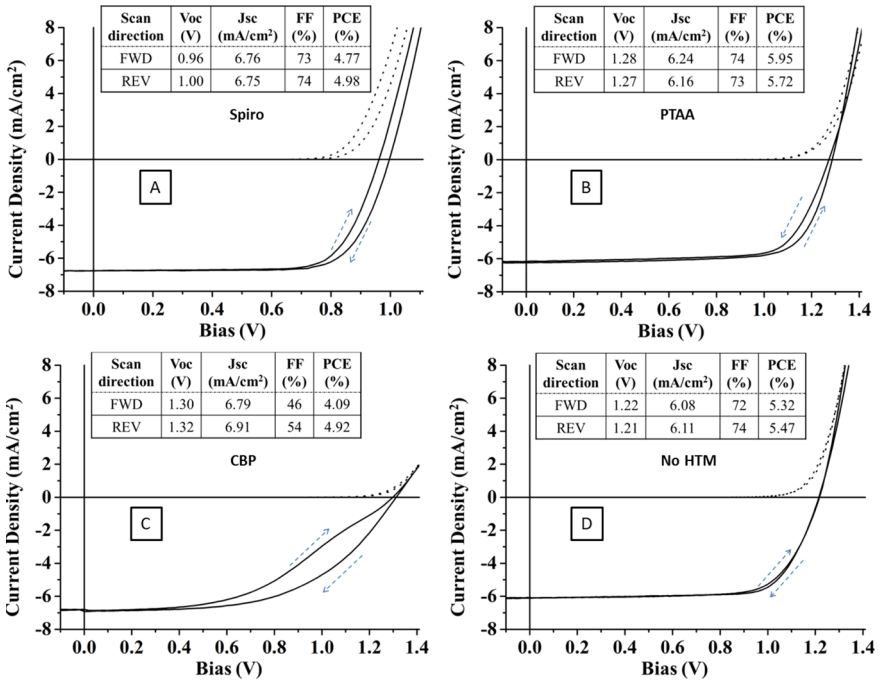

Figure 3. Light and dark $I-V$ plots of mp-TiO_2/$CsPbBr_3$ cells with the different HTMs as labeled (A–C) and without any HTM (D) (100 mW/cm^2 simulated solar irradiation, masked cell area 0.16 cm^2). Scan rate was 0.06 V/s.

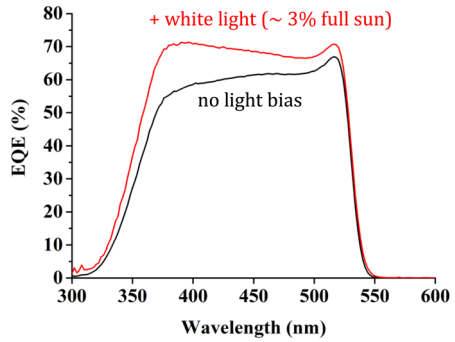

Figure 4. External quantum efficiency (EQE) spectral response of the $CsPbBr_3$/PTAA cell from Figure 3B with and without light bias.

Using CBP as the HTM, a much higher V_{OC} is expected (again based solely on the HOMO level of the CBP). Only a modest increase in this parameter was obtained, but the FF decreased considerably (Figure 3C). Also the hysteresis was much more prominent than in the previous cells. From our UPS measurements, done separately for the individual components, the CBP HOMO/$CsPbBr_3$ offset should be much less than for the other HTM/$CsPbBr_3$ interfaces −0.27 eV (5.97–5.7 eV as noted above), instead of 0.8–0.9 eV. Taking into account that these values are only indicative, it is possible that the rate of hole transfer across the perovskite/CBP interface is considerably slower than at the other perovskite/HTM interfaces, resulting in a hole buildup in the perovskite which would increase charge recombination (although we note that it does not affect the photocurrent at or close to zero bias). It may also be related to the higher series resistance of the CBP cell compared to the other HTM cells (a shallower slope of the high forward bias I–V characteristic), suggesting improvement might follow from higher doping of the CBP. This result is a further example that the commonly observed hysteresis is not merely a function of the perovskite bulk properties but is dependent also on the perovskite interfaces with other phases.

We also made cells without any HTM (Figure 3D). There have been a couple of reports of $MAPbBr_3$ cells made without a HTM with conversion efficiencies reaching 2% and V_{OC} up to 1.35 V.[15,16] With $CsPbBr_3$ we succeeded in obtaining HTM-free cells almost as good as our best cells with PTAA. Figure 3D shows the IV characteristics of such a cell, which is virtually hysteresis-free and with a performance that is only slightly inferior to that of cells with PTAA, mainly due to the somewhat lower V_{OC}.

Cells on mp-Al_2O_3 instead of on TiO_2 normally give a considerably higher V_{OC}.[10,16,17] As noted above, the mp-TiO_2 cells were much better than similar cells using mp-Al_2O_3. Up to now, the best cells using mp-Al_2O_3 are with spiro, with an overall efficiency of nearly 1.9%; however, the V_{OC} was, as expected higher (by >300 mV) at 1.33 V. The highest V_{OC} we obtained was using Al_2O_3 without any HTM, where we obtained >1.4 V (overall cell efficiency 1%). Current–voltage plots of these cells are shown in Figure S3 in the SI.

The fact that we have not (up to now) succeeded in fabricating cells on Al_2O_3 or planar cells comparable in performance with the mp-TiO_2 cells suggests that the transport properties of our $CsPbBr_3$ are still far from optimal. Because single crystals of the same material have shown excellent transport properties,[4] there is likely much room for improvement here.

To compare the above cells with hybrid $CH_3NH_3PbBr_3$ cells described in the literature, we have listed the hybrid cells in Table S1 in the Supporting Information. The important cell structure parameters are given since these have a strong effect on the cell performance, as does the electron transport material (TiO_2, either planar or planar + mesoscopic, or planar TiO_2 covered by mesoscopic Al_2O_3) and the HTM material.

Overall, the $CsPbBr_3$ cells compare well with the $MAPbBr_3$ cells in the table. The cell by Heo et al.[18] in the SI is

DOI: 10.1021/acs.jpclett.5b00968
J. Phys. Chem. Lett. 2015, 6, 2452–2456

outstanding and separate from all other cells and is not far from the theoretical maximum efficiency (the V_{OC} is the only parameter that might be increased appreciably), but up to now, 8 months after that work was published, we are aware of only one recent paper by Sheng et al.[19] with results that even begin to approach that value (and show a value of J_{SC} that is equivalent to an EQE of ~100%).

The all-inorganic halide perovskites have both disadvantages and advantages compared to the hybrid analogues. The most obvious disadvantage is the relatively high cost of Cs compared to the organic A cations (medium purity CsBr costs in the order of $1/g for 100−1000 g quantities). However, we note that Cs is far from being a rare element (it is more earth-abundant than Sn, to give a relevant comparison), and its present high cost is more a function of the low level of use than an intrinsic value. Also, while there are only two organic A cations that can presently be used in good halide perovskite-based cells, that is still twice the (present) number of suitable inorganic A cations. The availability of both increases the choice substantially. On the plus side, the all-inorganic compounds are certainly much more temperature stable than the hybrid analogues (e.g., we anneal the $CsPbBr_3$ films at 250 °C in air (see below), and the Cs component will not be lost by sublimation, although the resulting perovskites are still water-sensitive. The purpose of this Letter is not to suggest that all-inorganic cells will be better than hybrid cells (or for any other application that these compounds may be used in), but that

- the organic moiety is not an essential component *a priori*, particularly in obtaining high V_{OC} values, something that was not obvious up to now and is important for the fundamental science point of view, and
- useful comparative studies between hybrid organic−inorganic and all-inorganic metal halide perovskites can now be done.

EXPERIMENTAL METHODS

FTO transparent conducting substrates (Xinyan Technology TCO-XY15) were cut and cleaned by sequential 15 min sonication in warm aqueous alconox solution, deionized water, acetone, and ethanol, followed by drying under N_2 stream. A compact ~60 nm thin TiO_2 layer was then applied to the clean substrate by spray pyrolysis of a 30 mM titanium diisopropoxide bis(acetylacetonate) (Sigma-Aldrich) solution in isopropanol using air as the carrier gas on a hot plate set to 450 °C, followed by two step annealing procedure at 160 and 450 °C, each for 1 h in air.

A 500 nm-thick mesoporous TiO_2 scaffold was deposited by spin coating a TiO_2 nanoparticle (P25) paste onto the dense TiO_2 coated substrates. Two grams of TiO_2 P25 (Evonik) was mixed with 0.34 mL of acetic acid, 0.85 mL of deionized water, and 22 mL of ethanol, followed by sonication for 30 min. Then 3.58 mL of α-terpineol, 0.1 g of 46 cP ethyl cellulose, 0.1 g of 10 cP ethyl cellose were mixed with 6.1 mL of ethanol and finally added to the suspension. The paste was spin-coated for 5 s at 500 rpm and 40 s at 4000 rpm, followed by a two-step annealing procedure at 160 and 450 °C, each for 1 h in air.

The $CsPbBr_3$ films were prepared by a 2-step sequential deposition technique. 1 M of $PbBr_2$ (Sigma-Aldrich) in DMF was stirred on a hot plate at 75 °C for 20 min. It was then filtered using a 0.2 μm pore size PTFE filter and immediately used. The solution was spin-coated on preheated (75 °C) substrates for 1 min at 2500 rpm and was then dried on a hot plate at 75 °C for 30 min. After drying, the substrates were dipped for 10 min in a heated (50 °C) solution of 15 mg/mL CsBr (Sigma-Aldrich) in methanol for 10 min, washed with 2-propanol, dried under N_2 stream and annealed for 10 min at 250 °C. All procedures were carried out in an ambient atmosphere. The HTMs, Spiro-OMETAD (Borun Chemical), PTAA (Lumtec) and CBP (American Dye Source) were applied by spin-coating 3 s at 500 rpm followed by 40 s at 2000 rpm. The Spiro-OMETAD, PTAA and CBP solutions contained 100, 30, 40 mg of each HTM, respectively, in 1 mL of chlorobenzene, mixed with 10, 15, 3.6 μL of *tert*-butylpyridine and 31, 15, 7 μL of 170 mg/mL LiTFSI [bis(trifluoromethane)sulfonamide (in acetonitrile)], respectively.

The samples were left overnight in the dark in dry air before 100 nm gold contacts were thermally evaporated on the back through a shadow mask with 0.24 cm^2 rectangular holes.

Transmission and reflection of films were measured using a Jasco V-570 spectrophotometer equipped with an integrating sphere. Transmission was corrected for reflection by using $T_{corr} = T/(1 - R)$.

A Leo Ultra 55 scanning electron microscope was used for SEM imaging.

XRD measurements were conducted on a Rigaku ULTIMA III operated with a Cu anode at 40 kV and 40 mA. The measurements were taken using a Bragg−Brentano configuration through a 10 mm slit, a convergence Soller 5° slit and a Ni filter.

The $J-V$ characteristics were measured with a Keithley 2400-LV SourceMeter and controlled with a Labview-based, in-house written program. A solar simulator (ScienceTech SF-150) equipped with a 1.5AM filter and calibrated with a Si solar cell IXOLAR High Efficiency SolarBIT (IXYS XOB17−04 × 3) was used for illumination. The devices were characterized through a 0.16 cm^2 mask. The $J-V$ characteristics were taken after light soaking for 10 s at open circuit and at a scan rate of 0.06 V/s. We note that variation of the scan rate between 0.06 V/s and 1 V/s made no difference to the $J-V$ characteristics (measured for the PTAA cell).

External quantum efficiency/spectral response EQE was measured with a Thermo Oriel monochromator with the light chopped at 10 Hz. Current was measured using a Oriel Merlin and TTI PDA-700 photodiode amplifier. EQE was calculated by referencing to the spectral response of a Si photodiode with a known EQE.

UPS measurements were carried out using a Kratos AXIS ULTRA system, with a concentric hemispherical analyzer for photoexcited electron detection. UPS was measured with a helium discharge lamp, using He I (21.22 eV) and He II (40.8 eV) radiation lines. The total energy resolution was better than 100 meV, as determined from the Fermi edge of an Au reference sample.

ASSOCIATED CONTENT

Supporting Information

Tauc plots, XRD, $J-V$ plots of mp-Al_2O_3 cells, table of hybrid $MAPbBr_3$ or $FAPbBr_3$ photovoltaic cells together with a list of HTMs used for comparison with the $CsPbBr_3$. The Supporting Information is available free of charge on the ACS Publications website at DOI: 10.1021/acs.jpclett.5b00968.

DOI: 10.1021/acs.jpclett.5b00968
J. Phys. Chem. Lett. 2015, 6, 2452−2456

AUTHOR INFORMATION

Corresponding Authors

*E-mails: gary.hodes@weizmann.ac.il.
*E-mails: david.cahen@weizmann.ac.il.

Notes

The authors declare no competing financial interest.

ACKNOWLEDGMENTS

We thank Dr. Tatyana Bendikov for the UPS experiments. This work was supported by the Leona M. and Harry B. Helmsley Charitable Trust, the Sidney E. Frank Foundation through the Israel Science Foundation, the Israel Ministry of Science, and the Israel National Nano-Initiative. D.C. holds the Sylvia and Rowland Schaefer Chair in Energy Research.

REFERENCES

(1) Stoumpos, C. C.; Malliakas; Kanatzidis, M. G. Semiconducting Tin and Lead Iodide Perovskites with Organic Cations: Phase Transitions, High Mobilities, and Near-Infrared Photoluminescent Properties. *Inorg. Chem.* **2013**, *52*, 9019−9038 and references therein.

(2) Chen, Z.; Wang, J. J.; Ren, Y.; Yu, C.; Shum, K. Schottky Solar Cells Based on $CsSnI_3$ Thin-Films. *Appl. Phys. Lett.*, **2012**, *101*.

(3) Kumar, M. H.; Dharani, S.; Leong, W. L.; Boix, P. B.; Prabhakar, R. R.; Baikie, T.; Shi, C.; Ding, H.; Ramesh, R.; Asta, M.; et al. Lead-Free Halide Perovskite Solar Cells with High Photocurrents Realized Through Vacancy Modulation. *Adv. Mater.* **2014**, *26*, 7122−7127.

(4) Stoumpos, C. C.; Malliakas, C. D.; Peters, J. A.; Liu, Z.; Sebastian, M.; Im, J.; Chasapis, C.; Wibowo, A. C.; Chung, D. Y.; Freeman, A. J.; et al. Crystal Growth of the Perovskite Semiconductor $CsPbBr_3$: A New Material for High-Energy Radiation Detection. *Cryst. Growth Des.* **2013**, *13*, 2722−2727.

(5) Work on controlled direct comparisons of identically prepared Cs- and MA-$PbBr_3$-based cells is ongoing. At present, our one-step $MAPbBr_3$ cells are considerably better than the two-step ones in spite of their less-homogeneous morphology.

(6) Schulz, P.; Edri, E.; Kirmayer, S.; Hodes, G.; Cahen, D.; Kahn, A. Interface Energetics in Organo-Metal Halide Perovskite-Based Photovoltaic Cells. *Energy Environ. Sci.* **2014**, *7*, 1377−1381.

(7) Ryu, S.; Noh, J. H.; Jeon, N. J.; Kim, Y. C.; Yang, W. S.; Seo, J.; Seok, S. I. Voltage Output of Efficient Perovskite Solar Cells with High Open-Circuit Voltage and Fill Factor. *Energy Environ. Sci.* **2014**, *7*, 2614−2618.

(8) Choi, K.; Kwak, J.; Lee, C.; Kim, H.; Characteristic, K.; Kim, D.-Y.; Zentel, R. Thin Films of Poly-Triarylamines for Electro-Optic Applications. *Polymer Bull.* **2008**, *59*, 795−803.

(9) Zhang, T.; Liang, Y.; Cheng, J.; Li, J. A CBP Derivative as Bipolar Host for Performance Enhancement in Phosphorescent Organic Light-Emitting Diodes. *J. Mater. Chem. C* **2013**, *1*, 757−764.

(10) Edri, E.; Kirmayer, S.; Cahen, D.; Hodes, G. High Open-Circuit Voltage Solar Cells Based on Organic-Inorganic Lead Bromide Perovskite. *J. Phys. Chem. Lett.* **2013**, *3*, 897−902.

(11) Shi, D.; Adinolfi, V.; Comin, R.; Yuan, M.; Alarousu, E.; Buin, A.; Chen, Y.; Hoogland, S.; Rothenberger, A.; Katsiev, K.; et al. Low Trap-State Density and Long Carrier Diffusion in Organolead Trihalide Perovskite Single Crystals. *Science* **2015**, *347*, 519−522.

(12) Dong, Q.; Fang, Y.; Shao, Y.; Mulligan, P.; Qiu, J.; Cao, L.; Huang, J. Electron-Hole Diffusion Lengths > 175 mm in Solution-Grown $CH_3NH_3PbI_3$ Single Crystals. *Science* **2015**, *347*, 967.

(13) Fahrenbuch, A. L.; Bube, R. H. *Fundamentals of Solar Cells*; Academic Press: New York, 1983; pp 236−240.

(14) Kedem, N.; Brenner, T. M.; Kulbak, M.; Schaefer, N.; Levcenco, S.; Levine, I.; Abou-Ras, D.; Hodes, G.; Cahen, D. Light-Induced Increase of Electron Diffusion Length in a p-n Junction Type $CH_3NH_3PbBr_3$ Perovskite Solar Cell. *J. Phys. Chem. Lett.* **2015**, DOI: 10.1021/acs.jpclett.5b00889.

(15) Aharon, S.; Cohen, B. E.; Etgar, L. Hybrid Lead Halide Iodide and Lead Halide Bromide in Efficient Hole Conductor Free Perovskite Solar Cell. *J. Phys. Chem. C* **2014**, *118*, 17160−17165.

(16) Dymshits, A.; Rotem, A.; Etgar, L. High Voltage in Hole Conductor Free Organo Metal Halide Perovskite Solar Cells. *J. Mater. Chem. A* **2014**, *2*, 20776−20781.

(17) Suarez, B.; Gonzalez-Pedro, V.; Ripolles, T. S.; Sanchez, R. S.; Otero, L.; Mora-Sero, I. Recombination Study of Combined Halides (Cl, Br, I) Perovskite Solar Cells. *J. Phys. Chem. Lett.* **2014**, *5*, 1628−1635.

(18) Heo, J. H.; Song, D. H.; Im, S. H. Planar $CH_3NH_3PbBr_3$ Hybrid Solar Cells with 10.4% Power Conversion Efficiency, Fabricated by Controlled Crystallization in the Spin-Coating Process. *Adv. Mater.* **2014**, *26*, 8179−8183.

(19) Sheng, R.; Ho-Baillie, A.; Huang, S.; Chen, S.; Wen, X.; Hao, X.; Green, M. A. Methylammonium Lead Bromide Perovskite-Based Solar Cells by Vapor-Assisted Deposition. *J. Phys. Chem. C* **2015**, *119*, 3545−3549.

DOI: 10.1021/acs.jpclett.5b00968
J. Phys. Chem. Lett. 2015, 6, 2452−2456